IL NUOVO CIMENTO **48 C** (2025) 169
DOI 10.1393/ncc/i2025-25169-y

COMMUNICATIONS: SIF Congress 2024

Characterization of an extended gas target for the $^{22}\mathrm{Ne}(\alpha,\mathrm{n})^{25}\mathrm{Mg}$ project at LUNA

M. VAGNONI(1)(2)(*)

(1) *Università della Campania "Luigi Vanvitelli" - Caserta, Italy*
(2) *INFN Roma 1 - Roma, Italy*

received 18 February 2025

Summary. — The $^{22}\mathrm{Ne}(\alpha,\mathrm{n})^{25}\mathrm{Mg}$ reaction is one of the main neutron sources for the nucleosynthesis of heavy elements and its reaction rate is known with an high uncertainty at relevant astrophysics energy, so a new investigation of this nuclear reaction is necessary. The LUNA Collaboration is studying this reaction at the Bellotti Ion Beam Facility (IBF) installed at Gran Sasso National Laboratory (LNGS) in the framework of the ERC Starting Grant called Scintillator-He3 Array for Deep-underground Experiments on the S-process (SHADES). The main goals are the measurement of the cross-section in the low-energy range 600–800 keV and the redetermination of the resonance energy and strength at $E_\mathrm{R} = 830$ keV. To achieve the goal of a precision better than 10% in the cross-section measurement, a direct and precise characterization of the extended gas target is required. In this proceeding the gas target density profile measurement is described through the study of the $^{22}\mathrm{Ne(p,}\,\gamma)^{25}\mathrm{Mg}$ narrow resonance.

1. – Introduction

The $^{22}\mathrm{Ne}(\alpha,\mathrm{n})^{25}\mathrm{Mg}$ reaction is, together with the $^{13}\mathrm{C}(\alpha,\mathrm{n})^{16}\mathrm{O}$ reaction, the main neutron source for main s-process in Asymptotic Giant Branch (AGB) stars and the major source of neutrons for weak s-process in massive stars [1]. The astrophysical models of the two different components of s-process inside stars have uncertainties, especially in comparison with the solar abundance distribution for heavier elements [2].

Several experimental campaigns were performed by Stuttgart group at Dynamitron accelerator using an extended gas target [3-5], they measured the resonance at $E_\mathrm{R} = 830$ keV, but they obtained only upper limit data in the energy range of astrophysical interest due to a high level of neutrons from cosmic rays. To solve this issue, a new experimental campaign at an underground laboratory is necessary to significantly reduce the background from cosmic rays and achieve the goal of a precise measurement of the $^{22}\mathrm{Ne}(\alpha,\mathrm{n})^{25}\mathrm{Mg}$ cross-section.

(*) On behalf of the LUNA Collaboration.

The SHADES (Scintillator-He3 Array for Deep-underground Experiments on the S-process) ERC-project([1]), in the framework of the LUNA Collaboration, aims to directly measure the ^{22}Ne$(\alpha, \mathrm{n})^{25}$Mg cross-section in the low energy range (600–800 keV) with highly improved sensitivity over the state of the art by taking advantage of the natural shielding at the underground Gran Sasso National Laboratory (LNGS).

A dedicated gas target characterization is of crucial importance to obtain a cross-section measurement with a precision below 10%, as required by different astrophysical theories [6]. In the following, the gas target characterization is explained in details describing the dedicated experimental setup, the Narrow Resonance Technique used to investigate the beam heating effect, the data analysis and some previous results.

2. – Experimental setup and methods

The SHADES experiment is installed along the second beam line of the new 3.5 MV accelerator at LNGS, called the Bellotti Ion Beam Facility (BIB), which provides an intense α beam with a maximum current of 500 μA [7]. The experimental setup consists of an extended windowless gas target with a recirculation system for the enriched ^{22}Ne gas. The target chamber is surrounded by a high-efficiency array composed of 6 liquid scintillators and 18 ^{3}He counters used to detect neutrons.

An intense ion beam changes the gas temperature and pressure by interacting with the target particles and the ion energy loss produces a local beam heating: the beam heating effect. This effect could generate a relevant change of the gas target density, so a gas target characterization is mandatory [8]. The Narrow Resonance Technique is used to characterize the SHADES windowless gas target by studying the ^{20}Ne$(\mathrm{p}, \gamma)^{21}$Na reaction ($Q = 2432$ keV) and its narrow resonance at $E_{\mathrm{R}} = 1168.3 \pm 0.4$ keV([2]) with $\Gamma = 15.75$ eV and $\omega\gamma = 0.94 \pm 0.04$ eV [9]. The excited level energy is located at $E_{\mathrm{X}} = 3544$ keV and it de-excites to the ground state with a branching ratio of 99%.

A dedicated setup for the characterization is installed along the extended gas target (220 mm effective length) as shown in fig. 1. It is composed of a $LaBr_3$ scintillator positioned on a movable platform on one side of the chamber and surrounded by a 5 cm thick lead shielding with a 3 cm aperture in front of the detector itself. The platform could be moved at 14 different steps, that correspond to particular positions inside the target chamber. The windowless gas target is filled with natural Ne instead of enriched ^{22}Ne gas for limiting the expensive procurement, but they have the same chemical characteristics. While the beam is impinging on the gas, the resonance is realized in a precise position, that changes for different beam energies, allowing the gas density analysis at different position inside the target chamber.

3. – Data analysis and results

The data analysis is based on the calculation of the yield obtained from the number of signal events extracted under the peak at $E_\gamma = 3455$ keV, normalized by the total charge, after subtracting possible background events. The sources of background for the ^{20}Ne(p, $\gamma)^{21}$Na reaction can be related to natural background, intrinsic detector background and beam-induced background. The natural background is composed by environmental

([1]) ERC-StG SHADES, No. 852016.
([2]) The energy is expressed in the laboratory frame, otherwise it is explicated.

Fig. 1. – On the left, the scheme of the extended gas target for the SHADES experiment. A $LaBr_3$ scintillator on a movable table on one side of the target chamber surrounded by lead shielding. On the right, a photo of the experimental setup at the Bellotti Ion Beam Facility.

background, produced by radioactive products of the decay chains of ^{40}K, ^{238}U and ^{232}Th, and cosmic radiation, reduced by the natural shielding of 1400 m dolomite rock (3800 m of equivalent water) at LNGS underground laboratory, where the muon flux and the neutron flux are reduced of 6 and 4 orders of magnitude, respectively [10]. The intrinsic detector background is composed of $LaBr_3$ scintillator radioactive isotopes, like ^{138}La, which decays into ^{138}Ce, and ^{227}Ac, which is part of ^{235}U decay chain. A background spectrum, overlapped to a high statistics spectrum of the ^{20}Ne(p, γ)^{21}Na reaction, both normalized in time, is shown in fig. 2.

From the analysis, one can conclude that the intrinsic background of $LaBr_3$ detector and the beam-induced background did not influence the region of interest. The number of background events are evaluated by selecting two regions, one on the left and the other on the right side of the peak of interest (ROI). The beam-induced background looks differently if focusing on "on-resonance" position or on "off-resonance" position and so two different background models have been used. For the "on-resonance" spectrum, an exponential function is used (fig. 3):

$$f_{\mathrm{R}} = Ne^{-ax} + k, \tag{1}$$

while, for the "off-resonance" spectrum, a polynomial function is used (fig. 3):

$$f_{\mathrm{NR}} = p_4x^4 + p_3x^3 + p_2x^2 + p_1x + p_0. \tag{2}$$

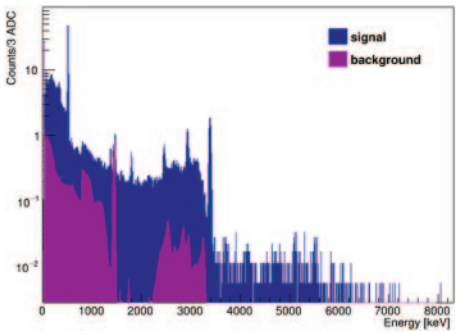

Fig. 2. – Overlap of signal spectrum with background spectrum. The signal spectrum is the one in blue and the background spectrum is the one in violet. The background spectrum breaks down below 3 MeV, so it does not influence the peak of interest at $E_\gamma = 3.5$ MeV.

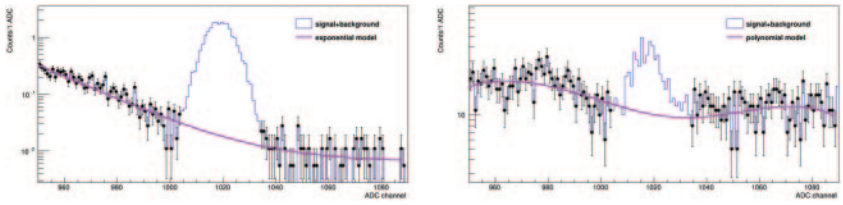

Fig. 3. – Signal spectrum: black points are selected to make the best-fit only in the lateral region of the region of interest, the best-fit is in purple. On the left the "on-resonance" spectrum and on the right the "off-resonance" spectrum.

The number of background events (B) are extracted integrating the best-fit background model in the region of interest, then the number of signal events (S) is obtained subtrahend B to the total number of events (N), obtained integrating the histogram in the ROI. The yield at each position along the gas target is calculated using S and the total charge (Q_{tot}):

$$Y = \frac{S}{Q_{\text{tot}}}. \tag{3}$$

The experimental yield as a function of position is obtained calculating the yield value for each detector position along the beam path analyzing each γ-spectrum acquired.

Figure 4 shows resonance scan profiles with compatible beam current, I_{beam}, and pressure, p, but different beam energies, E_{beam}. As expected by the beam energy loss, the position of the resonance goes from the entrance collimator up to the exit collimator by increasing the beam energy. Moreover, the yield profiles with higher beam energy are also more broaden and with a lower maximum yield value than the others and this effect is due to the beam straggling.

The yield as a function of detector position is analyzed using the theoretical yield defined as [11]

$$Y(E_0) = \int_0^{x_{\max}} \mathrm{d}x \int_{E_0}^{0} f(E, E(x))\, \sigma_{\text{BW}}\, \eta(x)\, \rho(x)\, \mathrm{d}E, \tag{4}$$

where E_0 is the beam energy, $x_{\max}$ is the target length, $\rho(x)$ is the gas density, $\eta(x)$ is the detector efficiency, σ_{BW} is the Breit-Wigner cross-section and $f(E, E(x))$ is the straggling distribution function, defined as a Gaussian distribution with $\sigma_{\text{beam}} \simeq 0.1$ keV and σ_{straggle}, that is defined according to the Bohr approximation:

$$\sigma_{\text{straggle}} = 1.20 \times 10^{-12} \sqrt{Z_{\text{p}}^2 Z_{\text{t}} \frac{\Delta E}{\epsilon}}, \tag{5}$$

where Z_{p} is the projectile particle charge, Z_{t} is the target particle charge, ΔE is the total energy loss and ϵ is the stopping power simulated by SRIM [12]. The efficiency function is parametrized using the Placeholder model as a first approximation, because the efficiency simulation is still in progress.

The gas density is extracted from the best-fit on data using the theoretical yield in eq. (4). An example of best-fit on data is shown in fig. 5, where the analyzed yield profile

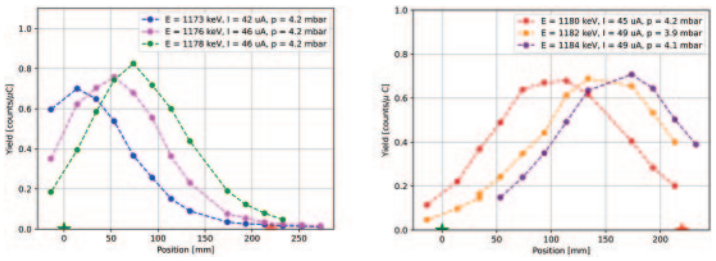

Fig. 4. – Yield as a function of detector position. The yield profile have similar beam currents and pressures, but different energies. The green star represents the entrance collimator of the target chamber and the red star the exit one. The dotted line are only to guide the eye along each profile.

has beam energy of $E_{\text{beam}} = 1176$ keV, beam current of $I_{\text{beam}} = 46.2$ μA and averaged gas pressure of $p = 4.15$ mbar.

Preliminary results of the gas density for three yield profiles with similar pressures and beam currents, but different energies are shown in table I.

The uncertainty on beam energy is of 0.1 keV, on beam current is of 2%. The uncertainty on gas pressure is dominated by systematic effect due to fluctuations during a complete scan data acquisition and this uncertainty is up to 7%. This uncertainty affects also the extracted gas density.

As shown in table I, the gas densities extracted in different positions of the gas target chamber are compatible, considering not only the statistics uncertainty, but also the systematic effects due to pressure fluctuations. Consequently, the gas target is homogeneous and also reproducible due to the fact that each complete scan was realized in different periods.

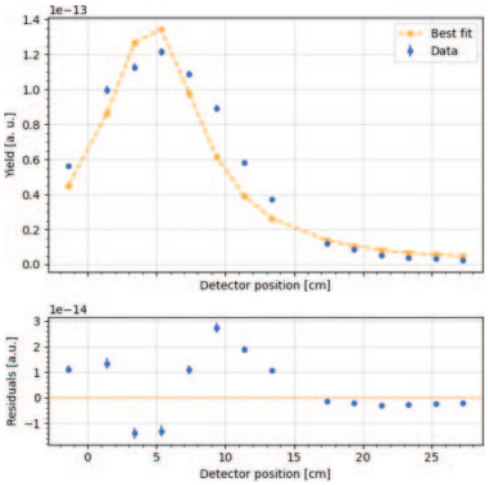

Fig. 5. – Best-fit on data of yield as a function of detector position. The experimental data are in blue and the best-fit curve in orange. In the x-axis there is the position and the y-axis there is the yield in arbitrary units.

TABLE I. – *Table with measurements of beam energy $E_{\rm beam}$, beam current $I_{\rm beam}$, gas pressure p, position where the resonance is populated $x_{\rm R}$ and preliminary gas density extracted with a best-fit on data ρ. The pressure value is the average of different values obtained during the complete scan of the resonance due to some pressure fluctuations.*

$E_{\rm beam}$ [keV]	$I_{\rm beam}$ [μA]	p [mbar]	$x_{\rm R}$ [cm]	ρ [atoms cm^{-3}]
1173	42.0	4.27	1.40 ± 0.05	$(2.699 \pm 0.024) \times 10^{17}$
1176	46.2	4.15	5.33 ± 0.05	$(2.482 \pm 0.015) \times 10^{17}$
1178	45.6	4.15	7.38 ± 0.05	$(2.273 \pm 0.008) \times 10^{17}$

4. – Conclusion

The SHADES gas target characterization is an important step to achieve a precise ^{22}Ne$(\alpha,\mathrm{n})^{25}$Mg cross-section measurement. The gas target characterization is studied using the Narrow Resonance Technique, in particular the resonance at $E_{\rm R} = 1168$ keV of the ^{20}Ne$(\mathrm{p},\gamma)^{21}$Na reaction. In this preliminary analysis, the gas target densities extracted at different positions inside the gas target for similar experimental conditions ($E_{\rm beam}$, $I_{\rm beam}$ and p) are confined within the 7%.

The beam-induced background is of the same order of the natural and intrinsic background, so all the materials used to build the gas target system are radiopure. Therefore, the SHADES gas target has optimal characteristics to achieve a precision below the 10% in the cross-section measurement of ^{22}Ne$(\alpha,\mathrm{n})^{25}$Mg reaction.

* * *

The authors acknowledge the support of INFN-Napoli Mechanical Service for the construction of the experimental setup. The authors are greatly indebted to the LNGS Accelerator Service for the support during beam time. This work has been funded by the European Commission (ERC-StG 2019 No. 852016).

REFERENCES

[1] ADSLEY P. *et al.*, *Phys. Rev. C*, **103** (2021) 015805.
[2] PIGNATARI M. *et al.*, *Nucl. Phys. A*, **758** (2005) 541.
[3] HARMS V. *et al.*, *Phys. Rev. C*, **43** (1991) 2849.
[4] DROTLEFF H. W. *et al.*, *Astrophys. J.*, **414** (1993) 735.
[5] JAEGER M. *et al.*, *Phys. Rev. Lett.*, **87** (2001) 202501.
[6] LONGLAND R. *et al.*, *Phys. Rev. C*, **85** (2012) 065809.
[7] JUNKER M. *et al.*, *Front. Phys.*, **11** (2013) 1291113.
[8] GORRES J. *et al.*, *Nucl. Instrum. Methods Phys. Res.*, **177** (1980) 295.
[9] LYONS S. *et al.*, *Phys. Rev. C*, **97** (2018) 065802.
[10] BEST A. *et al.*, *Eur. Phys. J. A*, **52** (2016) 1.
[11] ILIADIS C., *Nuclear Physics of Stars*, (John Wiley and Sons) 2015.
[12] ZIEGLER J. F. *et al.*, *Nucl. Instrum. Methods Phys. B*, **268** (2010) 1818.